Observational Study

Medicine®

OPEN

Morphobiochemical diagnosis of acute trabecular microfractures using gamma correction Tc-99m HDP pinhole bone scan with histopathological verification

Yong-Whee Bahk, PhD, MD[a], Seok-Ha Hwang, PhD, MD[b], U-Young Lee, PhD, MD[c], Yong-An Chung, PhD, MD[d,*], Joo-Young Jung, PhD[e], Hyeonseok S. Jeong, PhD[d]

Abstract

We prospectively performed gamma correction pinhole bone scan (GCPBS) and histopathologic verification study to make simultaneous morphobiochemical diagnosis of trabecular microfractures (TMF) occurred in the femoral head as a part of femoral neck fracture.

Materials consisted of surgical specimens of the femoral head in 6 consecutive patients. The specimens were imaged using Tc-99m hydroxymethylene diphosphonate (HDP) pinhole scan and processed by the gamma correction. After cleansing with 10% formalin solution, injured specimen surface was observed using a surgical microscope to record TMF. Morphological findings shown in the photograph, naive pinhole bone scan, GCPBS, and hematoxylin-eosin (H&E) stain of the specimen were reciprocally correlated for histological verification and the usefulness of suppression and enhancement of Tc-99m HDP uptake was biochemically investigated in TMF and edema and hemorrhage using gamma correction.

On the one hand, GCPBS was able to depict the calcifying calluses in TMF with enhanced Tc-99m HDP uptake. They were pinpointed, speckled, round, ovoid, rod-like, geographic, and crushed in shape. The smallest callus measured was 0.23 mm in this series. On the other hand, GCPBS biochemically was able to discern the calluses with enhanced high Tc-99m HDP uptake from the normal and edema dipped and hemorrhage irritated trabeculae with washed out uptake.

Morphobiochemically, GCPBS can clearly depict microfractures in the femoral head produced by femoral neck fracture. It discerns the microcalluses with enhanced Tc-99m HDP uptake from the intact and edema dipped and hemorrhage irritated trabeculae with suppressed washed out Tc-99m HDP uptake. Both conventional pinhole bone scan and gamma correction are useful imaging means to specifically diagnose the microcalluses naturally formed in TMF.

Abbreviations: CT = computed tomography, DICOM = digital information and communications in medicine, FWHM = full-width at half-maximum, GCPBS = gamma correction pinhole bone scan, H&E = hematoxylin-eosin, HDP = hydroxymethylene diphosphonate, MRI = magnetic resonance imaging, PXM = pixelized method, ROI = region-of-interest, TMF = trabecular microfractures.

Keywords: gamma correction pinhole bone scan, morphobiochemical diagnosis, trabecular microfracture

1. Introduction

Trabecular microfracture (TMF) of cancellous bone is ubiquitous, occurring in association with osteoporosis,[1] contusion,[2] aseptic ostoeonecrosis,[3] inflammatory, metabolic, and neoplastic diseases of bone,[4] and even normal physiological activity.[5,6] Its clinical effect may be negligible when localized. However, if systemic or widespread, it may become a condition to disturb the equilibrium state of the whole skeletal system manifesting not only as a major debilitating disease but also as a serious welfare and socioeconomic problem, in particular in the aged population.[7] TMF heals by producing microcallus, an aggregation of woven bone, manifesting as a "nodular, fusiform, angulated, or arched bridge lesion". [5] Scintigraphically, pinhole scan reveals Tc-99m hydroxymethylene diphosphonate (HDP) to avidly accumulate in microcalluses and is enhanced by gamma correction, whereas it is weakly accumulated in edema or hemorrhage irritated trabeculae and easily suppressed out.[4] Histopathologically, trabecular fractures are either complete and well defined or incomplete and poorly defined (Fig. 1, bottom panel).

TMF began to draw attention of researchers in the early 1960s as they were found in the necrotized femoral head in patients with hypercortisonism.[3] In the beginning, TMF was investigated using conventional radiography and then magnetic resonance imaging (MRI) came into use. The value of MRI for the diagnosis of TMF was first reported by Yao and Lee.[8] They observed high

Editor: Gaurav Malhotra.

The authors have no conflicts of interest to disclose.

Supplemental Digital Content is available for this article.

[a] Department of Nuclear Medicine, [b] Department of Orthopedics, Sung-Ae General Hospital, [c] Department of Anatomy, Catholic Institute for Applied Anatomy, [d] Department of Radiology, Incheon St. Mary's Hospital, [e] Biomedical Engineering and Research Institute, College of Medicine, The Catholic University of Korea, Seoul, South Korea.

[*] Correspondence: Yong-An Chung, Department of Radiology, Incheon St. Mary's Hospital, The Catholic University of Korea, #56 Dongsu-ro, Bupyeong-gu, Incheon 21431, South Korea (e-mail: nm@catholic.ac.kr).

Medicine (2017) 96:45(e8419)

Received: 11 October 2016 / Received in final form: 27 June 2017 / Accepted: 30 September 2017

http://dx.doi.org/10.1097/MD.0000000000008419

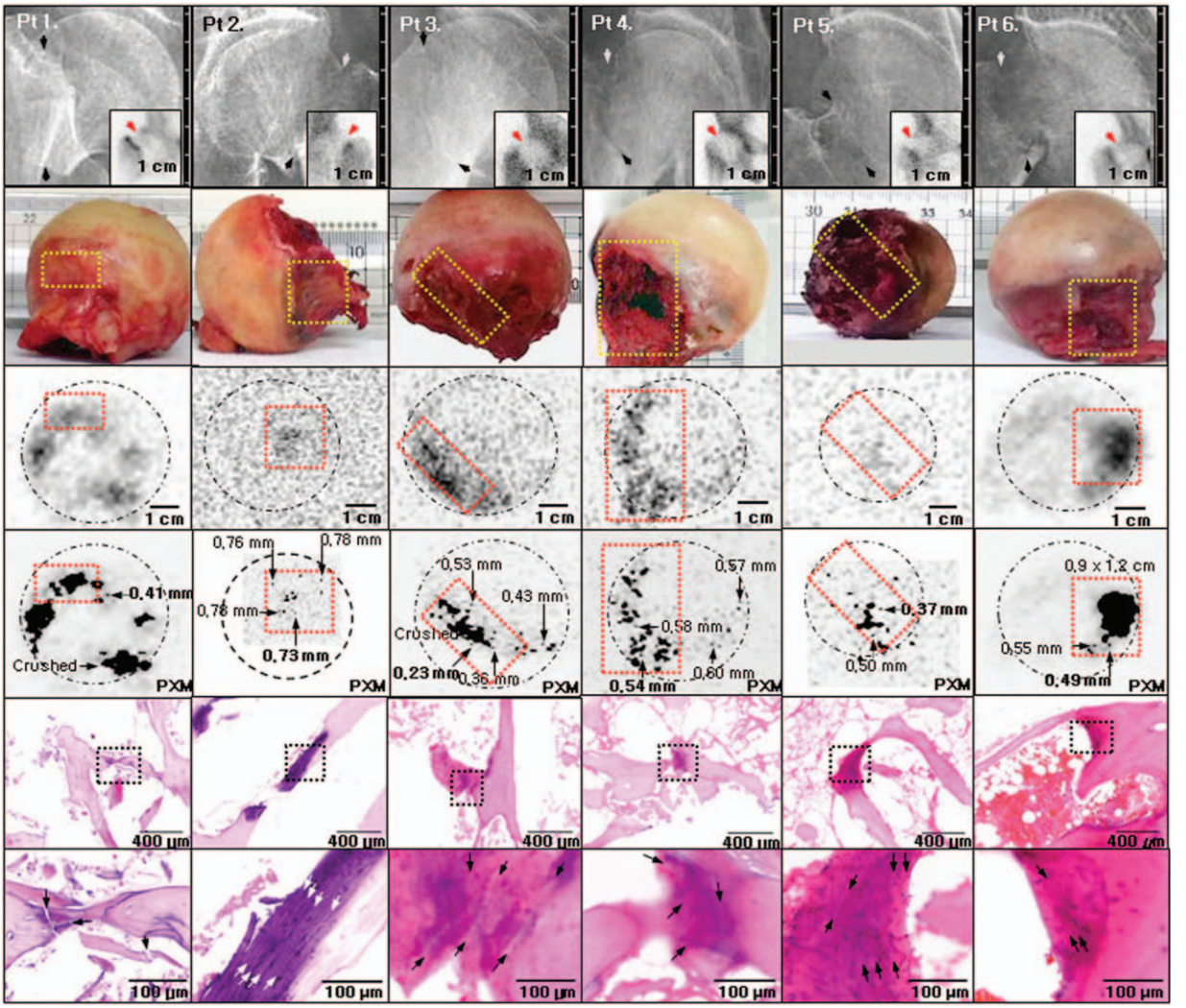

Figure 1. Patients, examinations, and results. [Top panel] Preoperative anteroposterior radiographs show femoral neck fracture with obvious osteoporosis (*arrowhead*). Inset is the preoperative pinhole scan showing avascular photopenia in femoral heads (*red arrows*). [Second panel] Fresh resected femoral heads show neck fracture with a ruler for basic measurement and region of interest (*frame*). [Third panel] Naive pinhole scans of specimen show ill-defined pathological and background Tc-99m hydroxymethylene diphosphonate (HDP) uptake (*frame*). [Fourth panel] Gamma correction pinhole bone scan (GCPBS) shows enhanced high tracer uptake in pinpoint, speckled, rod-like, geographic, and crushed fractures. Micro size was measured using the pixelized method (PXM). Crushed fracture contains micro lucency, but geographic fracture contains none. Note that the mild uptake in normal and edematous and/or hemorrhagic uptake is suppressed. [Fifth panel] Low power view (×40) hematoxylin-eosin (H&E) stain shows scanty trabecular microfractures with callus formation in porotic bone replaced by fat cells. Patient 6 shows hemorrhage. [Bottom panel] H&E stain (×100) shows linear microfractures in all patients. Fractures are well defined in Patients 1 to 3 and ill-defined in Patients 4 to 6 (*black arrows*). The definition of fracture seems unrelated with days of fracture.

signal intensity in the T2-weighted image and speckled or linear low signal intensity in the T1-weighted image in contused knee bones. These results were confirmed and furthered in a larger number of patients by Mink and Deutch.[9] On the other hand, Rangger et al[10] performed a histological investigation of microfractures of the cancellous bone using cryosection and Ryu et al[11] studied the MRI findings of bone contusion in swine. Recently, micro-computed tomography (micro CT)[12–14] and micro magnetic resonance imaging (micro MRI)[15,16] were developed for the three-dimensional imaging of TMF. In addition, our group found that Tc-99m HDP gamma correction pinhole bone scan (GCPBS) is useful to demonstrate the microcalluses in TMF[4,17] and it has been most recently verified histopathologically using rat experiment.[18]

Biochemically, GCPBS can discern TMF from intact trabeculae because the Tc-99m HDP uptake in TMF is enhanced by gamma correction, while the uptake in intact and edema or hemorrhage irritated trabeculae is suppressed.[4,17] Francis et al[19] published an important rat study noting high Tc-99m diphosphonates uptake to occur at sites of osteoneogenesis in acute healing fractures in Sprague-Dawley rats. They found that Tc-99m diphosphonates are more richly adsorbed onto the amorphous calcium phosphate which has more osteogenetic sites than the crystalline hydroxyapatite of normal bone. This combined histopathological and radiobiochemical study of ours was performed to prove that the morpho-biochemical diagnosis of actively calcifying calluses is possible using the principle of GCPBS.

2. Materials and methods

2.1. Surgical specimens from human subjects

We used surgical specimens of devascularized femoral heads removed for the treatment of femoral neck fracture recruited

from 6 patients. The 6 patients individually agreed to and signed an informed consent for this clinical study, which was approved by the Institutional Review Board. The age of patients ranged from 72 to 92 years (mean = 78.4) including 3 males and 3 females. The fracture involved the right femoral neck in 5 patients and the left in 1 patient. The femoral head was surgically removed 3 to 7 days after fracture.

2.2. Preoperative diagnosis by radiography and Tc-99m HDP pinhole bone scan

Femoral neck fracture and avascular necrosis of the femoral head were confirmed in each patient by conventional radiography and Tc-99m HDP pinhole bone scan, respectively (Fig. 1: top panel and insets). The anteroposterior radiograph of the injured hip joint was taken 24 hours prior to surgery using an automatic radiographic machine (Siemens Axiom Aristo MX, Germany) and Tc-99m HDP pinhole bone scan was performed in succession using a gamma camera (Siemens E-cam signature, Germany). Radiographic exposure factors were 65 to 70 kVp, 35 to 40 mAs, and 100 cm source-image distance and the anterior pinhole scan factors were 925 to 1110 MBq (25–30 mCi) Tc-99m HDP, 7-min scan time, and 12-cm pinhole-aperture-to-object distance which uniformly covered whole large joints including the shoulder, hip, and knee in adult without significant distortion. Pinhole aperture size was 4 mm (Supplementary Fig. 1, http://links.lww.com/MD/B948)

2.3. Gamma correction pinhole scan of specimen and correlation of thereof and H&E stain findings for histopathological identification

Necrotized femoral head with a portion of the subcapital neck was removed by surgery in each patient for bipolar hemiarthroplasty 24 hours after the diagnostic confirmation of disease (Fig. 1, second panel). Injuries in the surface of specimen were surveyed using a common magnifying lens (Fig. 1, second panel), imaged using a pinhole scanner (Fig 1, third panel, Supplementary Fig 2, http://links.lww.com/MD/B948), and processed by gamma correction (Fig. 1, fourth panel). As a representative demonstration, a sectioned region of interest in the femoral head specimen of Patient 3 was scrutinized under a surgical microscope (OPMI pico, Carl Zeiss, Oberkochen, Germany) confirming that seed-pearl-like calluses have already been formed (Fig. 2E). In turn, the findings were meticulously correlated with those of GCPBS (Fig. 2F) and hematoxylin-eosin (H&E) stain (Fig. 2Ga, Gb) for histopathological identification. As anticipated, GCPBS showed variously shaped injured trabeculae with micro- and macro-tracer uptake. The radioactivity so detected was derived from the undecayed residua of the Tc-99m HDP given to each patient for 24-hour preoperative bone scanning. The amount of tracer, aperture-to-object distance, field of view size, and matrix size were 1.0 to 1.07 GBq (3.7–4.0 mCi), 12 cm, 14 × 14 cm, and 256 × 256, respectively. Those data were needed for mathematic calculation of pixelized measurement. Photons accumulated ranged from 14 to 23 Kilocounts and the specimen scan time from 10 to 30 minutes according to the strength of residual radioactivity.

2.4. Gamma correction pinhole bone scan

Gamma correction was performed to biochemically differentiate suppressed Tc-99m HDP uptake from enhanced uptake. Methodologically, the original naive pinhole scan of each specimen (Fig. 2C) was processed by gamma correction using a Photo Correction Wizard program of ACD Photo Editor (ACD systems, Miami, FL) to discern individual micro Tc-99m HDP uptake (Fig. 2D). The gamma value was increased to suppress uptake in normal and edema and/or hemorrhage dipped (but not injured) trabeculae so that microcalluses in TMF with high tracer

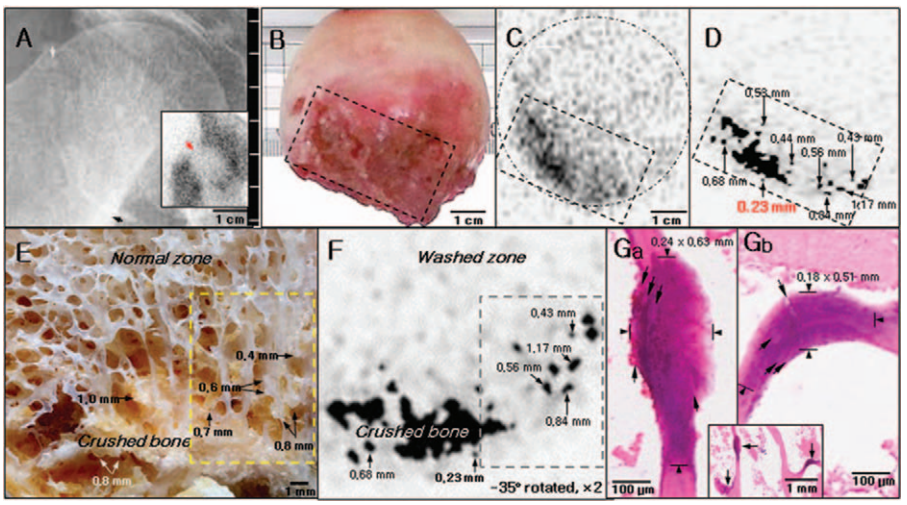

Figure 2. (Patient 3) A 3-day-old right femoral neck fracture with trabecular microfractures in a 72-year-old female. A, Anteroposterior radiograph of the right hip joint shows macro fracture (*arrows*). Inset is the preoperative pinhole scan showing avascularity in the femoral head (*red arrows*). B, Fresh surgical specimen shows injured bone surface (*frame*). C, Naive anterior pinhole scan shows Tc-99m hydroxymethylene diphosphonate (HDP) uptake in femoral head and subcapital neck (*frame*). The radioactivity derived from tracer administered to patients for 24-hour preoperative bone scan. D, Gamma correction shows enhanced pinpoint uptake in early healing calluses in trabecular microfractures and crushed bone. The smallest lesion was 0.23 mm as measured by pixelized measurement. E, Surgical microscopy (×10) shows variously sized calluses in microfractures and crushed bone (*arrows*). F, Gamma correction view is 35° counterclockwise rotated and 2-fold magnified so that gamma correction view is morphologically best compared with surgical microscope image. The size and shape of the Tc-99m HDP uptake in micro calluses in (E) and (F) (*frame*) are practically the same as those of hematoxylin-eosin (H&E) stain although all microfractures shown in (F) and (G) are not necessarily the same. Ga, Gb, H&E stains show 2 fusiform calluses (*arrowheads*) stained in reddish purple surrounding micro linear fractures (*long arrows*). Inset shows 3 microfractures (×20).

uptake kept enhanced. Gamma correction was processed by clicking the toolbars in the following sequence:[17] Exposure and autoexposure to maximize uptake intensity and done and save with a new name. Then, exposure and image-brightness control were done by increasing gamma value up to 95 starting from 50 (the default value) and done and save the finished image with another new name. The use of an original naive digital information and communications in medicine (DICOM) scan without any image modification was required.

2.5. Hematoxylin-eosin stain of calcifying calluses in trabecular microfractures

Each surgical specimen was decalcified and embedded in a paraffin block. The block was cut in 10-μm thickness using a rotary microtome (RM2255, Leica, Wetzlar, Germany). Then sections were scanned using a virtual microscope (OLIVIA, Olympus, Tokyo, Japan) and treated by H&E stain. For the better comparableness of microfracture finding, photomicrograph was 5-fold magnified (Fig. 2Ga, Gb).

2.6. Identification of trabecular microfractures in GCPBS and H&E stain

TMF heals by forming calcifying calluses, the sites of active osteoneogenesis, at which Tc-99m diphosphonates are dominantly adsorbed and fixed and remain enhanced by gamma correction.[17,18] Thus, GCPBS could recognize and identify TMF as such as pinpointed, speckled, round, ovoid, rod-like, and geographic high uptake (Fig. 1, fourth panel). Histopathologically, H&E stain studies were carried out in 2 steps. The first step was to find region-of-interest (ROI) using a low power view (Fig. 1, fifth panel) and the second step was to identify the calcifying calluses stained in base in the form of thready whitish microfractures closed up using a high-power view (Fig. 1, bottom panel and Fig. 2Ga, Gb). The reciprocal correlation of the findings of GCPBS and H&E stain permitted us to confirm that the calcifying calluses formed in TMF.

2.7. Quantification of microfracture tracer uptake using pixelized measurement

The size of individual micro Tc-99m HDP uptake was mathematically calculated using the pixelized measurement method.[20–22] Each micro-spot was appointed as a region of interest. The image profile is presented in a line spread function denoting the signal intensity of the applied line. The Y-axis of image profile is signal intensity and the X-axis shows the pixel number in profile. To easily measure the full-width at half-maximum (FWHM), matrix size was expanded to 512×512. Because of the increased number of pixels, the signal intensity value was assigned by interpolation at the expanded bin which does not have a signal intensity value. To interpolate the between bins, the Gaussian curve fitting method was used using the in-house MATLAB code (Mathworks, R2011a, USA).[20] The equation of the Gaussian curve fitting was as below.

$$y(x) = \frac{1}{\sigma\sqrt{2\pi}} \exp\left[-\frac{(x - x_0)^2}{2\sigma^2}\right]$$

y = interpolated value
x = original frame value
x0 = mean value of the frame value
σ = standard deviation

3. Results

3.1. Overall considerations

Six patients consisted of 3 males and 3 females with the age ranging from 72 to 92 years and a mean was 78.4 years. The causes of femoral neck fracture were falling down from a bed or chair or in a staircase or tumbling in toilet or street. The anatomical diagnosis of femoral neck fracture was made in each patient using plain radiography (Fig. 1, top panel proper) and radiobiochemical bone scan diagnosis of avascular necrotic femoral head by successive pinhole scan (Fig. 1, top panel inset). On the day next, the necrotized femoral head with a portion of the subcapital neck was removed by surgery to perform bipolar hemiarthroplasty (Fig. 1, second panel). Each femoral head specimen was surveyed immediately after removal using a reading glass (Fig. 1, second panel) and imaged using a pinhole scanner (Fig 1, third panel), and the pinhole scan was treated by gamma correction to discern TMF (Fig. 1, fourth panel). In the meantime, the injured surface of specimens was cleansed and scrutinized by a surgical microscope to confirm the formation of microcalluses (Fig. 2E) and finally the anatomical findings of individual microcalluses were compared with those of GCPBS and H&E stain for histological identification (Fig. 2F and Ga, Gb). TMF were presented as fine, whitish, thready shadows surrounded by basophilic stain. They were sharply, intermediately, or un-sharply defined (Fig. 1, bottom panel) and tended to be profuse in number. Some were meshy and granular in appearance (Fig. 2Ga, Gb).

3.2. Quantification of gamma correction pinhole bone scan and hematoxylin-eosin stain

The unprocessed naive pinhole scan of the specimen showed irregular areas of nebulous Tc-99m HDP uptake of various intensities which is not informative in terms of TMF (Fig. 1, third panel). The shape and size of such nebulous uptake could not be evaluated in any detail. However, the gamma correction suppressed out the blurred uptake in intact and edema and hemorrhage dipped trabeculae, now all distinctly revealing the microcalluses with high enhanced tracer uptake (Fig. 1, fourth panel). For quantification, the size of individual TMF was calculated using pixelized measurement (Fig. 2D). The smallest microcallus in Patients 1 to 6 was 0.41, 0.73, 0.23, 0.54, 0.37, and 0.49 mm (mean = 0.46 mm), respectively. The smallest pinpoint callus of all was 0.23 mm occurring in Patient 3 (Fig. 1, fourth panel). There were large crushed fractures with enhanced Tc-99m HDP uptake in Patients 1, 3, and 6. Fractures were completed in Patients 1, 2, and 3 and incomplete in Patients 4, 5, and 6. The difference was considered to be due to the different physical impact of trauma and the unequal nature and degree of callus formation. The surgical microscopic findings of many small seed-pearly microcalluses and crushed bone in Patient 3 (Fig. 2E) were in good accord with the pinpoint and crushed bone Tc-99m HDP uptake in GCPBS (Fig. 2F) and moderate accord was noted in all other patients. Low power H&E stain showed basophilic injured trabeculae in the bone marrow space with dominant fat cell filtration, fibrosis (patients 3–5), hemorrhage (patient 6), or effacement (patients 1 and 2).

3.3. Reciprocal correlation of shapes of tracer uptake and findings of surgical specimen, GCPBS, and H&E stain

The shape of the uptake was pinpointed, speckled, rod-like as well as crushed and geographic. Crushed fractures contained lucent microdefects, whereas compact geographic ones did not

(Patients 1 and 3 in Fig. 1, fourth panel). In general, the scrutiny and correlation of the findings shown in surgical specimen, GCPBS, surgical microscope, and H&E stain were in good accord individually and altogether, representing TMF (Figs. 1 and 2). In detail in Patient 3, for example, radiograph (Fig. 2A), surgical specimen (Fig. 2B), naive pinhole scan (Fig. 2C), GCPBS (Fig. 2D), surgical microscope (Fig. 2E), 3-fold magnified GCPBS (Fig. 2F), and H&E stain (Fig. 2Ga, Gb) showed neck fracture, femoral head surface injuries, nebulous Tc-99m HDP uptake, distinct pathological micro uptake, seed-pearly microcallus formation, whitish thready and meshy fractures with basophilic H&E stain, respectively. All these findings represented calcifying callus in TMF. Thus, GCPBS could diagnose TMF with pinpoint, speckled, rod-like, and geometric Tc-99m HDP uptake and crushed trabeculae (Fig. 2F). Furthermore, GCPBS distinguished the calcifying calluses in TMF with enhanced uptake from edema and hemorrhage dipped trabeculae with suppressed Tc-99m HDP uptake as far as trabeculae are not injured.

4. Discussion

TMF ubiquitously occur in a large variety of bone diseases[1–5] and even in normal physiological activity.[6,7] TMF is micro breakage of trabeculae which measures approximately 0.5 mm in thickness[1] and heals by callus formation. The callus is a micronodular aggregate of woven bone[1,6] and typically looks like a pearl seed (Fig. 2E). GCPBS is currently used for the micro anatomical diagnosis of occult fractures[17] and other bone diseases.[4] Besides, bone contusion incites endoblastic rimming to repair trabecular injury as confirmed by a recent rat experiment.[18] Gamma correction can distinguish the normal bone with mild Tc-99m HDP uptake and the edema and hemorrhage dipped bone with intermediary uptake from the actively forming callus with high enhanced uptake in fractured trabeculae. Such radiobiochemically different suppression of Tc-99m HDP uptake appears to be helpful for distinguishing bone edema, hemorrhage, TMF, and contusion. Recognizing the ever-increasing clinical and socioeconomic importance of TMF, new imaging tools are being actively developed, now including micro-CT[13] and multislice cone-beam CT[14] as well as the micro-MRI.[15,16]

We performed this combined bone scan imaging-histology study for 2 purposes using surgical specimens of traumatically devascularized femoral head recruited from 6 consecutive patients. The first aim was to histologically prove that GCPBS could precisely visualize and identify the active callus formed in TMF. The second aim was to biochemically confirm if gamma correction suppressed Tc-99m HDP uptake in normal bone and the edema and hemorrhage dipped trabeculae and contrarily preserves the enhanced high tracer uptake in the microcallus of TMF. Our results indicate that GCPBS can precisely identify calcifying calluses in TMF (Fig. 2E and F) and the high uptake in them is not suppressed out by gamma correction.

The size of the microcallus was measured using the pixelized method.[20–23] The function is an image profile that shows the signal intensity from the image matrix. Actually, the size was calculated by measuring the FWHM of the signal peak. The results of our gamma correction study revealed that the pinpoint and otherwise shaped Tc-99m HDP uptake shown on the surgical photomicrograph (Fig. 2E) and GCPBS (Fig. 2F) is in good accord, proving that the micro-uptake in gamma correction pinhole scan represents microcallus. Furthermore, the extended multicorrelation of findings of GCPBS, surgical microscope, and H&E stain likewise shows a good accord in morphology (Fig. 2).

To image trabecular microfractures, synchrotron radiation micro CT was used by Okazaki et al[13] obtaining a three-dimensional image of the microcallus in TMF in osteoporotic femoral head as we did in the current experiment. Our series was exclusively focused on the individual trabecula with microcallus which is distinctly imaged with enhanced high Tc-99m HDP uptake. The trabecular size ranged from 0.23 to 0.54 mm (n = 6; mean = 0.46 mm). It is to be mentioned that the pinhole scan of TMF by us is specifically confined to the bone forming callus, while the synchrotron radiation micro-CT visualizes trabecula and callus as a unit. A strong radiobiochemical advantage of GCPBS is that it can solely present a bone metabolic profile of microcalluses, rendering one to assess the healing state of the callus formed in TMF, possibly in both qualitative and quantitative manners.

In conclusion, GCPBS can simultaneously make the morphological and biochemical diagnosis of the actively calcifying calluses in TMF. The tiniest callus shown in our series was 0.23 mm in size. GCPBS can distinguish the microcalluses with enhanced higher Tc-99m HDP uptake from the inert and edema or hemorrhage dipped trabeculae with suppressed tracer uptake. GCPBS is an easily performed and economical imaging method to simultaneously provide useful morphological and biochemical information on the microcalluses formed in TMF.

Acknowledgment

This study was supported by a Grant of Global Frontier R&D Program on Human-centered Interaction for Coexistence (Ministry of Science and ICT, Republic of Korea, NRF-2012M3A6A3055707).

The authors acknowledge the graceful concern on this study of Dr Kim Yoon Kwang, the Chairman of Sung-Ae General Hospital, Seoul. The authors are also deeply indebted to Mr Woo Jin Chang for his expertise reference work and Mr Yong Hwan Kim, MI Application Specialist of Siemens/Korea, for his help in physics.

References

[1] Vernon-Roberts B, Pirie CJ. Healing trabecular microfractures in the bodies of lumbar vertebrae. Ann Rheum Dis 1973;32:406–12.
[2] Mandalia V, Henson JH. Traumatic bone bruising—a review article. Eur J Radiol 2008;67:54–61.
[3] McFarland PH, Frost HL. A possible cause for aseptic necrosis of the femoral head. Henry Ford Med Bull 1961;9:115–22.
[4] Bahk YW. Bahk YW. Combined scintigraphc and radilographic diagnosis of bone and joint diseases: including gamma correction interpretation. Gamma Correction Pinhole Bone Scan Diagnosis Springer Verlag, Berlin:2013;209–89.
[5] Fazzalari NL. Trabecular microfracture. Calcif Tissue Int 1993;53(suppl 1):S143–6.
[6] Frost HM. The spinal osteoporoses. Mechanisms of pathogenesis and pathophysiology. Clin Endocrinol Metab 1973;2:257–75.
[7] Tassani S, Matsopoulos GK. The micro-structure of bone trabecular fracture: an inter-site study. Bone 2013;60:78–86.
[8] Yao L, Lee JK. Occult intraosseous fracture: detection with MR imaging. Radiology 1988;167:749–51.
[9] Mink JH, Deutsch AL. Occult cartilage and bone injuries of the knee: detection, classification, and assessment with MR imaging. Radiology 1989;170:823–9.
[10] Rangger C, Kathrein A, Freund MC, et al. Bone bruise of the knee: histology and cryosections in 5 cases. Acta Orthop Scand 1998;69: 291–4.
[11] Ryu KN, Jin W, Ko YT, et al. Bone bruises: MR characteristics and histological correlation in the young pig. Clin Imaging 2000;24:371–80.
[12] Ito M. Recent progression in assessment of bone microstructure. Nihon Rinsho 2011;69:1233–8.

[13] Okazaki N, Chiba K, Taguchi K, et al. Trabecular microfractures in the femoral head with osteoporosis: analysis of microcallus formations by synchrotron radiation micro CT. Bone 2014;64:82–7.
[14] Klintstrom E, Smedby O, Moreno R, et al. Trabecular bone structure parameters from 3D image processing of clinical multi-slice and cone-beam computed tomography data. Skeletal Radiol 2014;43:197–204.
[15] Song HK, Wehrli FW. In vivo micro-imaging using alternating navigator echoes with applications to cancellous bone structural analysis. Magn Reson Med 1999;41:947–53.
[16] Rajapakse CS, Leonard MB, Bhagat YA, et al. Micro-MR imaging-based computational biomechanics demonstrates reduction in cortical and trabecular bone strength after renal transplantation. Radiology 2012; 262:912–20.
[17] Bahk YW, Jeon HS, Kim JM, et al. Novel use of gamma correction for precise (99m)Tc-HDP pinhole bone scan diagnosis and classification of knee occult fractures. Skeletal Radiol 2010;39:807–13.
[18] Bahk YW, Chung YA, Lee WY, et al. Gamma correction Tc-99m hydroxymethylene diphosphonate pinhole bone scan diagnosis and histopathological verification of trabecular contusion in young rats. Nucl Med Commun 2016;37:988–91.
[19] Francis MD, Ferguson DL, Tofe AJ, et al. Comparative evaluation of three diphosphonates: in vitro adsorption (C-14 labeled) and in vivo osteogenic uptake (Tc-99m complexed). J Nucl Med 1980;21: 1185–9.
[20] Yoon Dk, Jung JY, Hong KJ, et al. Tomographic image of prompt gamma ray from boron neutron capture therapy: a Monte Carlo simulation study. Appl Phys Lett 2014;104:083521.
[21] Yoon DK, Jung JY, Han SM, et al. Statistical analysis for discrimination of prompt gamma ray peak induced by high energy neutron: Monte Carlo simulation study 2015;303:859–66.
[22] Jung JY, Cheon GJ, Lee YS, et al. Pixelized measurement of Tc-99m HDPMicro particles formed in gamma correction phantom pinhole scan: a reference study. Nucl Med Mol Imaging 2016;50: 207–12.
[23] Miller AL, Schraer H. Ultrastructural observations of amorphous bone mineral in avian bone. Calcif Tissue Res 1975;18:311–24.